

S. Nalesso, C. Codemo, E. Franceschinis, N. Realdon, R. Artoni, A.C. Santomaso, Texture analysis as a tool to study the kinetics of wet agglomeration processes (2015) *International Journal of Pharmaceutics*, 485, 61-69.

DOI: <http://dx.doi.org/10.1016/j.ijpharm.2015.03.007>

Texture analysis as a tool to study the kinetics of wet agglomeration processes

Silvia Nalesso^a, Carlo Codemo^b, Erica Franceschinis^b, Nicola Realdon^b, Riccardo Artoni^c, Andrea C. Santomaso^{a,*}

^a*APTLab - Advanced Particle Technology Laboratory, University of Padova, Department of Industrial Engineering, via Marzolo 9, 35131 Padova, Italy*

^b*PharmaTeG - Pharmaceutical Technology Group, University of Padova, Department of Pharmaceutical and Pharmacological Sciences, via Marzolo 5, 35131 Padova, Italy*

^c*LUNAM Université, IFSTTAR, site de Nantes, MAST/GPEM, Route de Bouaye CS4, 44344 Bouguenais, France*

* corresponding author: tel. +39 049 8275491 email address: andrea.santomaso@unipd.it (Andrea C. Santomaso)

Abstract

In this work wet granulation experiments were carried out in a planetary mixer with the aim to develop a novel analytical tool based on surface texture analysis. The evolution of a simple formulation (300 g of microcrystalline cellulose with a solid binders pre-dispersed in water) was monitored from the very beginning up to the end point and information on the kinetics of granulation as well as on the effect of liquid binder amount were collected. Agreement between texture analysis and granules particle size distribution obtained by sieving analysis was always found. The method proved to be robust enough to easily monitor the process and its use for more refined analyses on the different rate processes occurring during granulation is also suggested.

Keywords: wet granulation, granulation kinetics, planetary mixer, texture analysis

1. Introduction

Wet granulation is a common pharmaceutical operation aiming at eliminating unfavorable properties of fine powders, improving flow properties, compaction characteristics and composition homogeneity of the granulated products. It is usually performed in four phases: (1) homogenization of dry powders; (2) liquid addition; (3) wet massing with liquid feeding system switched off; (4) granules drying. All these phases (excepted drying) are often carried out in mechanically agitated vessels which can promote efficient mixing also of cohesive materials. Such mixers exert an intense local shear on the powder which breaks down the small cohesive aggregates (Harnby, 1997), promotes a good liquid dispersion and a proper product consolidation (Cavinato et al., 2010). They are generally constituted by a vessel and an impeller rotating about an horizontal or a vertical axis. When rotating about a vertical axis, the impeller can also revolve following circular trajectories so that these mixer-granulators are called planetary or orbital mixers (Laurent, 2005; Hiseman et al., 2002). In some cases the rotating axis does not revolve but it is the vessel that rotates (Boerefijn et al., 2009). Despite the large use of this type of granulators in many industrial processes, the agglomeration mechanisms caused by liquid binder addition are currently not totally understood (Laurent, 2005; Knight et al., 2001). Granulation can be indeed affected by a large number of variables, including process parameters, material properties and formulation variables (Faure et al., 2001). Monitoring the behavior of a wet bed of powders and following its evolution during time is

of paramount importance to design, analyze and control the pharmaceutical manufacturing process in a Process Analytical Technology (PAT) perspective. Different techniques have been used in the past to monitor and carry out a description of the powder agglomeration process within the mixer-granulator. A comprehensive review of such techniques can be found in Watano (2001). Most of the measurement methods can give an indirect information on the status of the granulation process since they do not observe the particles directly but they measure physical variables supposed to be related to particle size. Acoustic emission, for example, has shown possibilities for granulation end-point detection (Briens et al., 2007). Also amperage or motor power consumption and impeller torque are frequently monitored as indirect measures of the agglomeration process. Particularly, power consumption and impeller torque have been used to identify how the system evolve during the agglomeration as a function of mixer geometric configuration (impeller and bowl shape) and impeller speed (Paul et al., 2003). Leuenberger et al. (2009) have investigated the relationship between granule growth and power consumption curves and have demonstrated the possibility of end-point determination by power consumption monitoring. Bier et al. (1979) also reported that records of power consumption and torque were in good agreement. In alternative to the end point determination Leuenberger et al. (2009), torque has been used also to predict the starting point of granulation (Cavinato et al., 2010, 2013) as a function of liquid binder amount. All this methods however, even if effective in collecting information about the process, are indirect; other techniques can give a more direct information on the status of the granules in the mixer-granulator. Techniques such as the focused beam reflectance measurement (FBRM), which allows to follow the granule chord length evolution in real time (Huang et al. 2010), are starting to be used in wet granulation studies. Also the simultaneous combination of different techniques such as FBRM, acoustic emission measurement and near infrared spectroscopy have been used to asses granulation rates in fluidized beds (Tok et al., 2008). A direct measurement and control of granule growth can be also achieved through the use of sensors capturing digital images of the powder bed and analyzing them with image analysis techniques. Image processing systems have been used for direct and continuous monitoring of the granule growth in fluidized bed granulation (Watano, 2001) and in high shear granulators (Watano et al., 2001). Since all the above techniques try to identify each particle individually, issues related to particles overlapping and contacts, and to the minimum number of particles to be analyzed exist. For process control purposes it would be advisable to develop PAT analyzers able to process thousand of particles simultaneously and extract averaged information on the status of the granular mixture during time, possibly providing real-time process information. Texture analysis (TA) of digital images of the powder bed surface (also known as surface imaging (Lakio et al., 2012)) can be potentially used in this sense. TA is already used in a variety of applications spanning from remote sensing to automated inspection and medical image processing (Russ, 1999; Gonzales et al., 2004). The basic idea behind the use of TA is that smooth surfaces will have small variation in gray scale values and the rougher the surface the larger are the variations. In the pharmaceutical context it has been used to determine the particle size distribution (PSD) (Laitinen et al., 2002) and the segregation tendency of granulated products (Lakio et al., 2012) in static conditions. In this work the wet granulation process was studied with TA by taking time series of digital images of the moving powder bed inside the granulator during the whole granulation process. The subsequent analysis was therefore carried out on the bulk powder (not on single

granules) and its evolution from being a dry mixture up to a wet mass of distinct aggregates was monitored and studied. The aim of the work was to assess if TA can be used as an analytical tool to observe the effect of different liquid binder addition rates and amounts on the granulation kinetics and on product properties.

The paper is structured as follows: in Section 2 some principles of image and texture analysis are resumed and the texture descriptors, the experimental set-up and the materials are presented. The potential of the texture analysis is verified and tested in Section 3 with preliminary experiments in simplified and controlled conditions. In Section 4 the use of TA is finally described in wet granulation experiments where the granulation kinetics are measured as a function of binder addition rate and the effects of binder total amount on granules PSDs are described.

2. Experiments and methods

2.1. Texture analysis

The main advantages of looking at surface texture are that the technique is not invasive and the particles are not analyzed individually but in bulk. Moreover issues on sample preparation, on the number of granules to be analyzed, on the dispersion of the material to avoid particles overlapping and contacts are therefore avoided. Since the camera can be positioned far enough from the moving powder bed, fouling of the lenses can be avoided as well. This allows to analyze a moving bed of particles provided that the surface is sufficiently defined and a suitable lighting source is available.

TA attempts to quantify intuitive qualities described by terms such as rough, smooth, silky or bumpy as a function of the spatial variation in pixel intensities on gray-scale digital images that in our case are pictures of the powder bed surface (Laitinen et al., 2002). A digital image (raster or bitmap image) is a binary representation of a two-dimensional image with a finite set of digital values, called picture elements or pixels. Pixels are ordered in a fixed number of rows and columns and hold a set of quantized values that represent the color and the brightness at any specific point. Often for scientific and industrial purposes digital images are in gray-scale i.e. only the brightness z_i (or intensity level) is given for each pixel (Russ, 1999; Gonzales et al., 2004). The index i indicates the level number which for a 8 bit image spans from 0 to $2^8 = 256$. Level intensities can be graphically represented according to their frequency of appearance in the image (number of pixels with a given intensity) as histograms $f(z_i)$. Two examples of intensity histograms are shown in Figure 1. They characterize two images of generic granules with different size. It can be appreciated also by simple visual inspection that the larger the granules size, the more contrasted the surface and the broader the corresponding histogram, i.e. $f(z_i)$ spreads over a larger number of intensity levels. It is therefore clear that a correlation between intensity level histogram, texture of the image and particle size exists and this correlation can be used to study the granulation process where changes in size of the wet aggregates occur.

Several texture descriptors of different complexity exist. In order of increasing complexity, we can enumerate descriptors based on the average value, the standard deviation (STD), the third moment of the intensity level histogram and those based on the gray level co-occurrence matrix (GLCM). GLCM is a second order statistics which describes the spatial correlation between couples

of neighbouring pixels by compiling the frequency for which different gray level intensities are found in a defined area (Gosselin et al., 2008). On the whole 11 descriptors have been considered but finally the standard deviation STD of $f(z_i)$ has been used in this study since most of the texture descriptors were found to be equivalent to STD (the same or similar information could be extracted). Similarly to other texture descriptors (such as smoothness, uniformity or entropy which implementation can be found in Gonzales et al., 2004) STD is based on some statistics performed on $f(z_i)$. In particular the STD in mathematical form is expressed as:

$$\sigma = \sqrt{\mu_2(z_i)} \quad (1)$$

and is related to the second moment, μ_2 , about the mean m of the histogram $f(z_i)$:

$$\mu_2 = \sum (z_i - m)^2 f(z_i) \quad (2)$$

From the observations and reasonings made on Figure 1 it is intuitable that the STD, which is recognized as a simple but robust measure of the average contrast of the image (Gonzales et al., 2004), has the potential for being used as an analytical tool in the granulation process.

2.2. Image Acquisition

Two different types of experiments were performed, static and dynamic tests, with increasing level of difficulty for the image acquisition process. Static tests were performed on small samples of granulated dry materials of known particle size and size distribution, in order to verify the feasibility of the TA in simplified conditions. Tests were performed in a simple ad hoc setup with controlled lightning conditions. It was a photographic box made of an open vertical PVC cylinder (150 mm in diameter and 200 mm long); the powder was put in a 25 cm³ cup (27.4 mm in diameter) placed at center of the cylinder base (Figure 2). The light source was constituted by a continuous strip of white LEDs fitted to the internal wall of the box to form a ring. A digital camera (DBK-61BUC02, 1/2" CMOS, 2048×1536, The Imaging Source, Bremen, Germany) with 12mm/1:1.4 lens (Pentax) and a 5 mm spacer was aligned on the top of the cylinder axis to take pictures of the sample surface.

In the dynamic tests the same camera was placed above the mixer vessel but for geometric constraints due to the arm holding the impeller, it was not axially positioned. Because of the offset only a portion of the bed surface was monitored. The image acquisition process was automated at a frame rate of 0.5 fps and with an exposure time of 1/714 s. A relatively short exposure time was required to avoid the blurring of the images due to the surface motion. As a consequence of the short exposure time of the CMOS sensor a more intense lightning of the surface was required. The light source was constituted by three continuous strips of white LEDs (instead of one as in the static experiments) fitted to form three rings. The rings were fixed to the mixer internal wall through a metallic structure (Figure 3). In both cases the height of the light source with respect to the powder surface was roughly 80-90 mm, while that of the camera was 290 mm.

Because of the orbital motion it could be that the impeller appeared in some of the images taken during the granulation experiments biasing the analysis. The upper part of the impeller was therefore painted green and pictures containing green pixels were automatically discarded by working in the HSV (hue, saturation and value) color-space where green was found in the range 0.3-0.4 of the hue channel (Dal Grande et al., 2008). The image selection procedure and the TA

were not performed on the full image but on a region of interest (ROI) of size 200 x 300 pixels. The resolution of the images was 105 $\mu\text{m}/\text{pixel}$, so that the observation area was 21.0 x 31.5 mm large. The size, the shape and the position of the ROI were chosen with a trial and error procedure in order to minimize the presence of the impeller blade in the pictures and consequently the number of discarded images during the analysis. On the average 15% of the images were discarded. After selection, the ROI was converted to gray-scale and processed by TA. All the softwares for image selection and for TA were customized and written in Matlab (MATLAB 7.5 and Image Processing Toolbox 6.0, The MathWorks, Inc., Natick, Massachusetts, United States). Image acquisition instead was performed with the software bundled with the digital camera (IC Capture v2.2).

2.3. Powders and granulating liquid

A simple formulation made up of microcrystalline cellulose (T1 Ph. Eur., MCC) was chosen as it is commonly used in pharmaceutical granulations and has porous particles able to absorb high amount of granulation liquid. The batch size was 300g. The MCC particle size, determined with Malvern Mastersizer 2000 (Worcestershire, 185 UK), expressed as d_{10} , d_{50} , d_{90} resulted equal to 13, 48 and 176 μm respectively.

Dispersion in water of xanthan gum (XG) at 0.05w/w% was used as liquid binder. XG is a polysaccharide produced by aerobic fermentation of glucose, sucrose or lactose by the bacterium *Xanthomonas campestris*. It is used as a pharmaceutical thickening agent and as a stabilizer and thickening agent in food preparations (E415) because of its strong thickening power (Litster and Ennis, 2004). In order to obtain the liquid binders, XG powder was pre-dispersed in water. In this way complications related to additional rate processes such as the hydration of the solid binder during the granulation process were avoided.

The viscosity of the binder aqueous dispersion was measured with a rotational viscometer (Rotovisco RV20, Haake, Germany) and the surface tension with the sessile drop method (Middlemann, 1995). Their values were respectively 30 mPa s and 0.069 N/m, while the density was 998.0 kg/m^3 .

MCC and XG powders were provided by ACEF SpA, Fiorenzuola d'Arda, Piacenza, Italy.

2.4. Granulation procedure

Experiments have been carried out in a planetary mixer (Kenwood Major Premier KMM 760, Kenwood Ltd., London, UK) which consisted of a bowl 200 mm high with 230 mm maximum diameter and 6.7 l total volume. A standard K shaped impeller was used. The mixer bowl was open at the top so that it was possible to observe the powder bed by visual or camera inspection during the granulation process and a sensor was used to collect digital images of the powder bed as described in Section 2.2. The mixer was operated at constant impeller speed of 100 rpm in all the experiments. The ratio between rotations and revolutions was fixed by a gearing ratio of 3.333. The working conditions were chosen in order to ease the development of the analytical method based on TA. A detailed description of this specific mixer geometry and of the flow patterns inside the mixer can be found in dedicated papers (Hiseman et al., 2002; Laurent, 2005).

The granulation procedure followed these steps: a) powder loading, b) dry mixing (3 minutes), c) wetting phase (with variable length from 4 to 36 minutes according to liquid binder

addition rate), d) massing phase (5 minutes), e) granules discharge and f) drying.

The liquid binder was added to the MCC using a peristaltic pump (Velp SP 311/2) by dripping from three evenly spaced points (droplet size was approximately 4 mm). The amount of liquid was fixed to 330 g excepted where specified. The feed flow rate adopted in the experiments were in the range 9 to 83 ml/min. The feed rate was monitored by measuring the decrease in weight of the liquid remaining in the reservoir (see Figure 3). Granules were then dried in a ventilated oven at temperature of 50°C overnight and sieved (AS 200 control Retsch, Germany) using the following sieves: 45, 100, 200, 300, 400, 500, 600, 710, 800, 1000, 1410, 2000, 5000 μm .

3. Results and discussion

Preliminary static tests (out of the mixer) and dynamic tests (within the mixer) were carried out in dry conditions in order to validate the TA and verify its ability to distinguish between powder mixtures made of particles with different sizes. This was of course a necessary prerequisite to develop an analytical method able to follow particle size variations in time as a consequence of liquid binder addition. It is important to emphasize here that no attempt were made to determine the full PSD of the granulation products with TA since this task is beyond the scopes of this work. In previous literature works full PSDs of granules have been measured with TA by using static samples under sequential bidirectional lightning (Laitinen et al., 2002; Lakio et al., 2012). The strictly controlled lighting conditions adopted in such works can not be obtained inside the mixer in dynamic conditions so that we limited the study to the use of a simple texture index, the STD, related to particle size in average sense.

3.1. Preliminary static tests

Two different tests were performed using static samples. The first test was made on monodispersed powders or granules. A granulated microcrystalline cellulose was sieved in 7 size ranges (spanning from 50 to 1000 μm). Images of bulk powder belonging to each size range were taken in the photographic box and surface texture was analyzed. The results in terms of STD of the gray-scale histogram are shown in Figure 4 where it can be appreciated that the STD increased monotonically with the granules size in a quite large size range. A second test was then made in order to verify if TA was effective also with polydispersed powder mixtures of smaller size (which is more similar to what can be found in a granulator especially in the early stages of the process). Different quantities of MCC particles ($d'_{50} = 75 \mu\text{m}$) and granules ($d'_{50} = 250 \mu\text{m}$) were mixed together in 8 different proportions (0, 0.1, 0.2, 0.4, 0.5, 0.6, 0.8, 1.0 expressed as fractions of the granules weight) and analyzed as previously described for the monodispersed case. Also in this case the TA was able to distinguish between different samples with a roughly linear trend of the STD as a function of the average particle size of the mixture calculated as $d'_{50} w + d'_{50} (1 - w)$, where w is the weight fraction of larger particles (Figure 5).

3.2. Preliminary dynamic tests

The observation of the powder bed surface in process conditions, i.e. within the mixer with impeller rotating at 100 rpm, was a more complex task than in static conditions. Many issues can

indeed affect the dynamic image acquisition:

- changes of distance between the powder bed surface and the CMOS sensor which occur during the granulation process when powder is moving or when becomes wet (focusing problems);
- particles in rapid motion (causing motion blurring in some portions of the image);
- uneven surface illumination (due to the impeller position, for example, which can generate shadows on the surface biasing texture identification);
- insufficient illumination (due to the reduced sensor exposure time, required to reduce motion blurring);
- impeller presence in the visual field (hindering the powder surface observation).

Optimal conditions for bed surface observation were therefore found through dedicated tests performed in dynamic conditions on 7 monodispersed MCC granulated particles (sizes from 100 to 3000 μm). The relationship between STD and particle size are reported in Figure 6. Also in this case a trend with the particle size was found. TA and in particular the use of STD demonstrated to be robust and reliable enough to follow and analyze the changes in size occurring in the planetary mixer. All the preliminary tests (static and dynamic) were successfully performed in different size ranges typical of the industrial granulation processes (from 75 to 3000 μm) suggesting therefore the possibility of developing an analytic tool able to follow the granulation process from the very beginning up to the end point.

3.3. Results from the process

The wet granulation experiments were carried out in the planetary mixer. In order to appreciate the agglomeration process Figure 7 reports some pictures of the powder surface at increasing time intervals. It is evident, even by simple visual inspection, that at minute 4 the surface becomes progressively rougher (liquid addition started at minute 3). This corresponded to an increase of the MCC particles cohesion mediated by capillary forces. The cohesion caused the particle to aggregate forming increasingly larger agglomerates, the enlargement process reached a maximum at 14 minutes and then the agglomerates started to reduce in size up to a final equilibrium value. It is interesting (and at the same time counterintuitive) to note that the size of the agglomerates started to reduce before the addition of liquid binder was stopped. Liquid addition stopped at minute 16 while the decrease in size started at minute 14 (i.e. 2 minutes before). This behavior is common to all the experiments so it is important, in this context, to verify if the proposed analytical tool, based on image analysis, was able to detect it. This was done by comparing the visual information of Figure 7 with the response of the TA. In Figure 8 the STD profile of the above experiment is reported as a function of time. The start and the stop time of liquid addition are represented in Figure as vertical dashed lines.

An increase in STD was expected after minute 3 and indeed, after an initial dry mixing step where STD remained constant at a minimum value, a linear increase of the profile was observed after starting liquid addition. The change of surface texture (quantified by an increase of image contrast) was therefore correctly detected by the STD and could be correlated to the progressive increase in size of the MCC agglomerates observed in Figure 7. At a given time (in this case

roughly at minute 12) STD reached a maximum and then started to decrease meaning that surface texture tended to homogenize because of a size reduction of the largest aggregates in the mixture. TA was therefore in complete agreement with the initial visual observation that the maximum size of the agglomerates was reached before the stopping of the liquid feeding. At the end of the process the STD profile tended to become flat meaning that an equilibrium between the different and competing agglomeration mechanisms was reached and size remained constant.

To assess the reliability of the method, the variability associated to the joint effects of the granulation experiments and of the TA was evaluated with replicated tests performed in the same conditions. Figure 9, shows the result of three replicated granulation tests carried out at 28 ml/min of binder flow rate. The average STD profile and the corresponding error bars (representing the standard deviation of STD at each monitored time) are reported. It can be observed that the variability of the STD was not constant during the process. It was minimum in the early stages of the process ($\pm 6\%$), then increased reaching a maximum before the STD peak ($\pm 12\%$) and then reduced towards the end where the profile tended to become flat ($\pm 6\%$). So even if the general trend of the STD profiles is clear, it happens that while the early stages and the end point of the granulation process can be characterized quite confidently by TA, attention should be paid looking at the central stage of the granulation process where STD variability is larger.

3.4. Effect of binder flow rate

In order to study the applicability of the TA on granulation kinetic studies experiments at different liquid binder flow rate (9, 22, 28, 47, 83 ml/min) were performed. The liquid binder was a dispersion of XG in water (0.05 w/w%).

Since the amount of liquid binder was fixed to 330 g so the duration of each experiment was different with the wetting phases lasting respectively 36, 15, 12, 7 and 4 minutes. Results are reported as STD profiles in Figure 10 where it is evident their strong dependence on the binder flow rate. In particular the following observations can be done:

- the overall shape of the profile did not change since they all showed a maximum of STD;
- the early stages of the process (nucleation and growth) were strongly influenced by the binder flow rate;
- the maximum of the STD (i.e. the maximum size of the wet agglomerates) was always reached before the stopping of the binder feeding (stopping time is not reported in the Figures for sake of clarity, it always occurred 5 minutes before the end of the granulation process because the massing time was a constant);
- the final level of the STD profiles (i.e. the final sizes of the wet agglomerates) were roughly constant, independent of the flow rate and of the process length;

A more detailed analysis can be carried out by quantifying the slope m of the profiles through two linear fittings performed before and after the maximum of STD (Figure 10: a and b respectively). Kinetic information are summarized in Figure 11 where the value of the kinetic constants (slopes of the linear fitting) are reported as function of the binder flow rate. It can be observed that while the growth rates increased with the binder flow rate, the size reduction rates were almost constant and independent of binder flow rate, which is consistent with the fact that the operating conditions were nearly the same in this stage of the process. This again indicates that TA response is sensitive to and

coherent with the physical changes of the system. Figure 12 instead shows the liquid to solid ratio, L/S , required to reach the maximum in the STD profiles (i.e. the maximum size of the agglomerates), as a function of binder flow rate. The evidence that when flow rate increases, the maximum granule size is reached with larger amount of liquid binder, suggests that a competition between liquid addition rate and liquid adsorption rate (by the MCC primary particles) exists. The second evidence that the size of the wet agglomerates starts to reduce before the liquid binder addition is stopped, suggests that also a competition between growth and breakage mechanisms exists. Since MCC particles are porous, the capillaries within the porous particles draw liquid into the interior of the particle, leaving at the surface less liquid available to form bridge bonds with other particles. If a sufficient fluid flow rate is used to saturate the MCC particles, or at least allow them to become surface wet, new MCC particles can be continuously incorporated into the granules. If however liquid addition rate is low, liquid will be completely absorbed into the MCC internal pores so that new liquid bridges can not form and the growth of the granules start to be contrasted by the breakage action of the impeller action already at low L/S ratios. Size reduction continues until an equilibrium granule size is reached where the strength of the aggregates equates the shear stresses generated by the impeller. This is a tentative explanation and the full understanding of the phenomena just described is beyond the scope of this paper which is focused on the development of an analytical tool.

In order to corroborate the idea that constant values of STD profiles at the end of the granulation process correspond to the same size of the wet agglomerates, the PSDs of the final dry granules were measured by sieving and as can be observed in Figure 13 they resulted to overlap, with $d_{50} = 680 \pm 50 \mu\text{m}$. The constant value of the final granule size however is not surprising if we think that, all the formulation variables (type of powder and liquid binder) and the operating conditions (impeller speed, powder amount, massing time), excepted for the binder flow rate, were the same in all the experiments.

Even though the history of the granules was very different (different residence time in the batch mixer, different duration of the growth and consolidation phases) the final PSDs were very similar. This observation in addition to the fact that all the experiments were carried out with the same impeller speed suggests the idea that experiments were operated in the so called mechanical dispersion regime (Hapgood et al., 2003). In the mechanical dispersion regime the final PSD is roughly independent of the liquid dispersion modality and wetting dynamics and depends mainly on the intensity of the mechanical agitation, that in our case was the same in all the experiments.

3.5. Effect of binder amount

In order to further validate the TA methodology a set of experiments was also performed by changing the total amount of liquid binder and keeping constant the binder addition time (12 minutes). Therefore the binder flow rate was changed together with the total amount of binder. With 330 g of binder, the flow rate was the same as in the previous experiments 28 ml/min while for 360 g of binder the flow rate increased to 30 ml/min. It can be observed that despite the very small flow rate variation a significant difference of liquid binder amount was added to the powder in the two cases ($\Delta = 30$ g of liquid binder on 300 g of MCC). The corresponding STD profiles are shown in Figure 14 where it can be observed that:

- the slope of the STD profiles is roughly constant (linear increase) up to minute 11 independently of the flow rate;
- large variability of STD profiles can be observed around minutes 12-13;
- clear differences of the STD profiles can be observed (after stopping liquid addition, i.e. during massing time) as a function of the total liquid binder amount;

It is clear from the Figure that a variation of binder flow rate as small as 2 ml/min in the early stages of the process can not be detected by the TA so that an overlap of the profiles was observed. The effect of the total binder amount on the final values of STD (end point of granulation) however was much larger so that significant size differences of the wet agglomerates were observed in the two cases. Again this observation was corroborated by the measurement of the final PSD (Figure 15). With 330 g of binder the granule d_{50} was $680 \pm 50 \mu\text{m}$, while for 360 g of binder the d_{50} was significantly higher $1615 \pm 115 \mu\text{m}$.

It has to be noted also that due to the different binder amount also the general trends of the STD profiles were slightly different. For lower binder amount (330 g) a clear maximum was always reached, followed by the decrease in size of the agglomerates (as already discussed). For the larger binder amount (360 g) instead the existence of a maximum in the STD was less evident and (because of the larger variability of the method in this phase of the process as reported in Figure 9) it was difficult to draw conclusions on the maximum size reached by the wet agglomerates in this stage of the process. It can be observed however that for larger binder amount the size reduction stage is nearly missing, which is physically coherent with the fact that an increased amount of liquid, added in the same time interval, can generate a larger number of capillary bridges and increase the strength of the agglomerates.

4. Conclusions

An analytical tool based on texture analysis was developed in order to follow the wet granulation process in a planetary mixer from the beginning up to the end point. Images of the powder surface within the mixer were captured during the granulation process and analyzed with several texture indexes. The standard deviation of their gray-scale histogram was selected to monitor the size evolution of the wet aggregates. The method was critically analyzed showing its applicability in granulation kinetic studies and in the investigation of the effects of formulation variables (here reduced for sake of simplicity to the liquid binder amount only). Texture analysis proved to have the ability to give an insight into several aspects of the granulation processes which of course need to be fully addressed in future contributions.

5. References

- Bier, H. P., Leuenberger, H., Sucker, H., 1979. Determination of the uncritical quantity of granulating liquid by power measurements on planetary mixers. *Pharm. Ind.* 41, 375–380.
- Boerefijn, R., Juvin, P. Y., Garzon, P., 2009. A narrow size distribution on a high shear mixer by applying a flux number approach. *Powder Technology* 189 (2), 172–176.
- Briens, L., Daniher, D., Tallevi, A., 2007. Monitoring high-shear granulation using sound

and vibration measurements. *International Journal of Pharmaceutics* 331, 54–60.

Cavinato, M., Andreato, E., Bresciani, M., Pignatone, I., Bellazzi, G., Franceschinis, E., Realdon, N., Canu, P., Santomaso, A. C., 2011. Combining formulation and process aspects for optimizing the high-shear wet granulation of common drugs. *International Journal of Pharmaceutics* 416, 229–241.

Cavinato, M., Artoni, R., Bresciani, M., Canu, P., Santomaso, A. C., 2013. Scale-up effects on flow patterns in the high shear mixing of cohesive powders. *Chemical Engineering Science* 102 (0), 1–9.

Cavinato, M., Bresciani, M., Machin, M., Bellazzi, G., Canu, P., Santomaso, A. C., 2010. Formulation design for optimal high-shear wet granulation using on-line torque measurements. *International Journal of Pharmaceutics* 387, 48–55.

Chirkot, T., Propst, C., 1997. Low shear granulators in Handbook of Pharmaceutical Granulation Technology. Marcel Dekker, New York, 1997, 205-225.

Dal Grande, F., Santomaso, A. C., Canu, P., 2008. Improving local composition measurements of binary mixtures by image analysis. *Powder Technology* 187(3), 205–213.

Ennis, B. J., 2006. Theory of granulation: an engineering perspective, in Parikh, D.M. (Ed.), Handbook of Pharmaceutical Granulation Technology, 2nd ed. Taylor and Francis Group, New York (U.S.A.), pp. 7-78.

Faure, A., York, P., Rowe, R., 2001. Process control and scale-up of pharmaceutical wet granulation processes: a review. *European Journal of Pharmaceutics and Biopharmaceutics* 52, 269–277.

Gonzales, R. C., Woods, R. E., Eddins, S. L., 2004. Digital Imaging Processing using Matlab. Pearson Prentice-Hall.

Ryan Gosselin, R., Duchesne, C., Rodrigue, D., 2008, On the characterization of polymer powders mixing dynamics by texture analysis, *Powder Technology* 183, 177-188.

Hapgood, K. P., Iveson, S. M., Litster, J. D., Liu, L. X., 2007, Granulation rate processes, in Salman, A.D., Hounslow, M.J., Seville, J.P.K. (Eds.) Granulation. Elsevier B.V., pp. 898–977.

Hapgood, K. P., Litster, J. D., Smith, R., 2003. Nucleation regime map for liquid bound granules. *AIChE J.* 49, 350–361.

Harnby, N., 1997. Mixing in the process industries. Butterworth-Heinemann, Oxford, UK.

Hiseman, M. J. P., Laurent, B. F. C., Bridgwater, J., Wilson, D. I., Parker, D. J., North, N., Merrifield, D. R., 2002. Granular flow in a planetary mixer. *Chemical Engineering Research and Design* 80 (5), 432–440.

Huang, J., Kaul, G., Utz, J., Hernandez, P., Wong, V., Bradley, D., Nagi, A., O'Grady, D., 2010. A pat approach to improve process understanding of high shear wet granulation through in-line particle measurement using fbrm c35. *Journal of Pharmaceutical Sciences* 99(7), 3205–3212.

Knight, P. C., Seville, J. P. K., Wellm, A. B., Instone, T., 2001. Prediction of impeller torque in high shear powder mixers. *Chemical Engineering Science* 56, 4457–4471.

Laitinen, N., Antikainen, O., Yliruusi, J., 2002. Does a powder surface contain all necessary information for particle size distribution analysis? *European Journal of Pharmaceutical Sciences* 17, 217–227.

Lakio, S., Hatara, J., Tervakangas, H., Sandler, N., 2012. Determination of segregation

S. Nalesso, C. Codemo, E. Franceschinis, N. Realdon, R. Artoni, A.C. Santomaso, Texture analysis as a tool to study the kinetics of wet agglomeration processes (2015) *International Journal of Pharmaceutics*, 485, 61-69.

DOI: <http://dx.doi.org/10.1016/j.ijpharm.2015.03.007>

tendency of granules using surface imaging. *Journal of Pharmaceutical Sciences* 101 (6), 2229–2238.

Laurent, B. F. C., 2005. Structure of powder flow in a planetary mixer during wet-mass granulation. *Chemical Engineering Science* 60 (14), 3805–3816.

Leuenberger, H., Puchkov, M., Krausbauer, E., Betz, G., 2009. Manufacturing pharmaceutical granules: Is the granulation end-point a myth? *Powder Technology* 189, 141–148.

Litster, J. D., Ennis, B., 2004. The science and engineering of granulation processes. Kluwer Powder Technology Series.

Middlemann, S., 1995. Modeling axisymmetric flows: dynamics of films, jets, and drops. Academic Press, Inc.

Paul, E. L., Atiemo-Obeng, V. A., Kresta, S. M. (Eds.), 2003. Handbook of Industrial Mixing: Science and Practice. Wiley-Interscience, John Wiley & Sons, Inc., Hoboken, New Jersey.

Russ, J., 1999. The Image Processing Handbook, 3rd Edition. Boca Raton, FL: CRC Press.

Tok, A. T., Goh, X., Ng, W. K., H., T. R. B., 2008. Monitoring granulation rate processes using three pat tools in a pilot-scale fluidized bed. *AAPS PharmSciTech* 9 (4), 1083–1091.

Watano, S., 2001. Direct control of wet granulation processes by image processing system. *Powder Technology* 117, 163–172.

Watano, S., 2007. Online monitoring, in Salman, A.D., Hounslow, M.J., Seville, J.P.K. (Eds.) Granulation. Elsevier B.V., pp. 478–498.

Watano, S., Numa, T., Miyanami, K., Osako, Y., 2001. A fuzzy control system of high shear granulation using image processing. *Powder Technology* 115, 124–130.

Figures

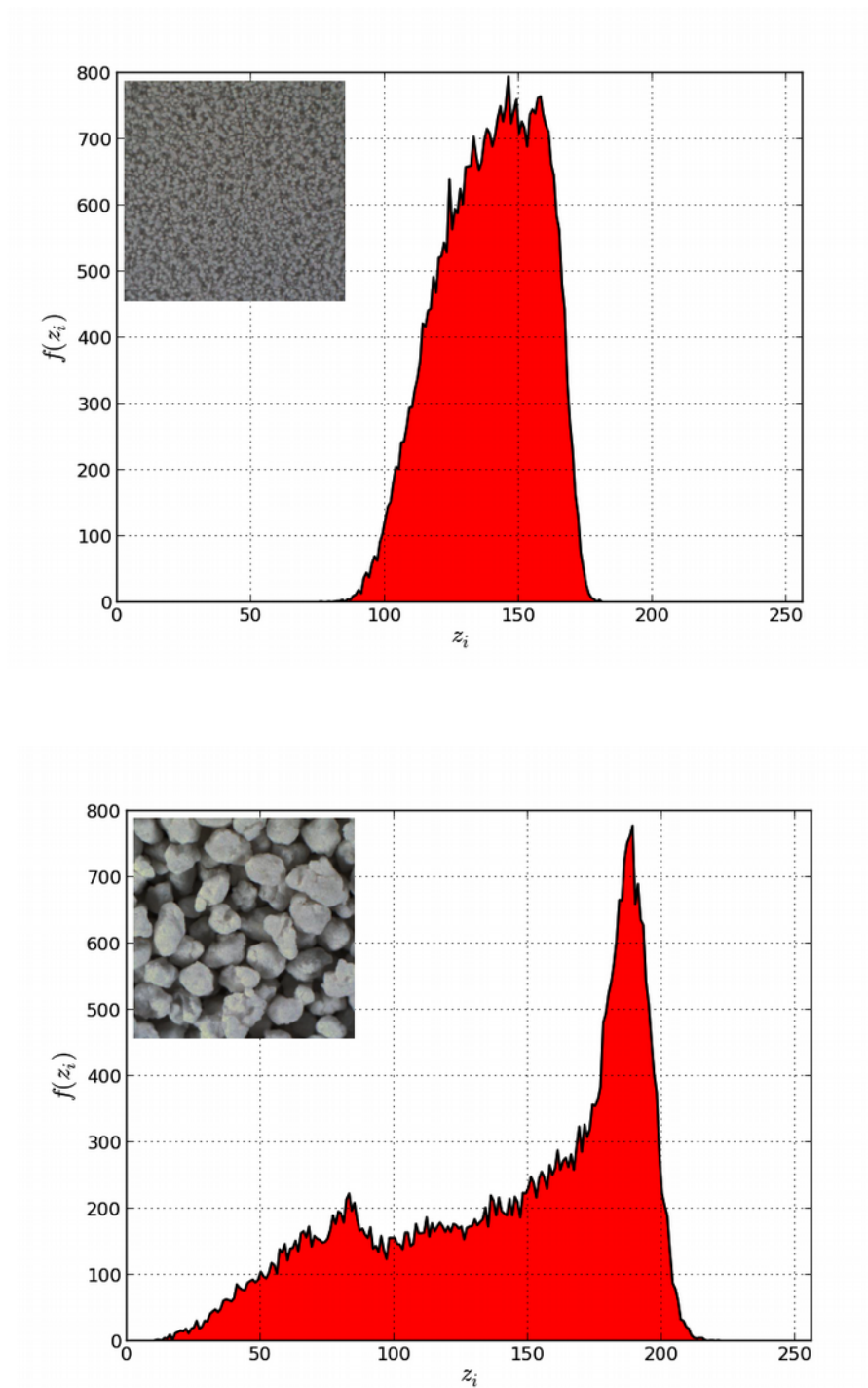


Figure 1: Example of histograms of intensity levels for two different particle sizes.

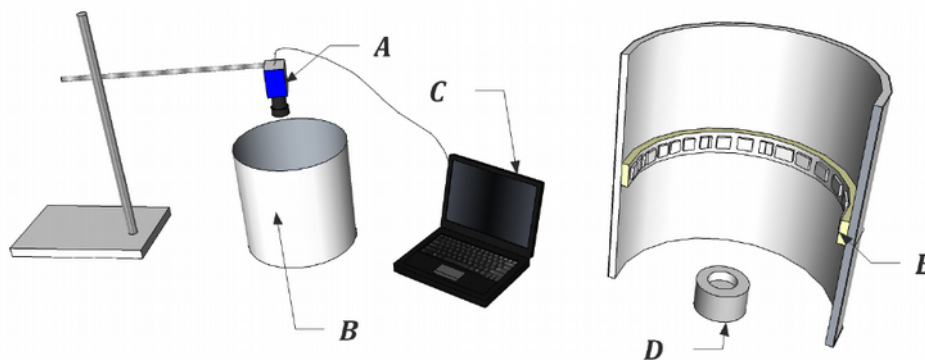


Figure 2: Experimental set-up for taking images from static samples. A) Digital camera. B) Photographic box containing the sample of powder protected from external light. C) Computer for image storage. D) Sample holder. E) The photographic box is represented magnified and sectioned to show the position of the sample holder and of the ring of LEDs.

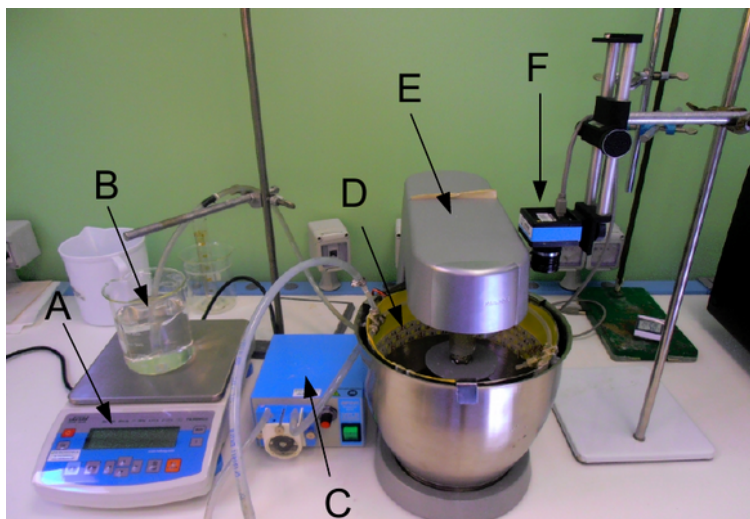


Figure 3: Experimental set-up for dynamic analysis of the granulation process. A) Electronic balance. B) Liquid binder dispersion. C) Peristaltic pump. D) Metallic circular structure holding three rings of LEDs for even illumination of the powder bed surface. E) Planetary mixer. F) Digital camera, connected to a frame grabber and a personal computer (not shown).

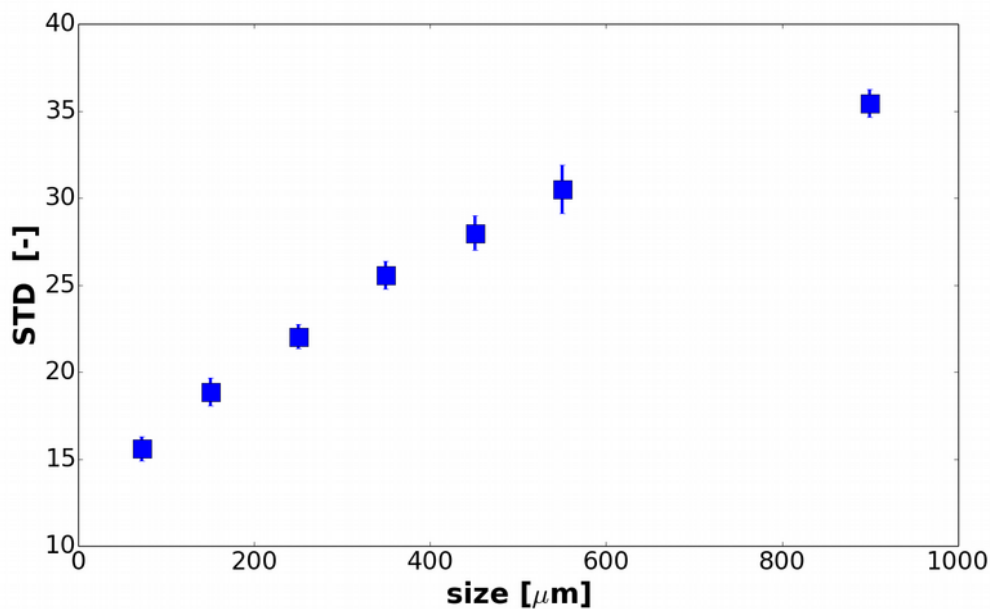


Figure 4: STD of the gray-scale histogram of the powder bed surface as a function of particle size (monodispersed samples).

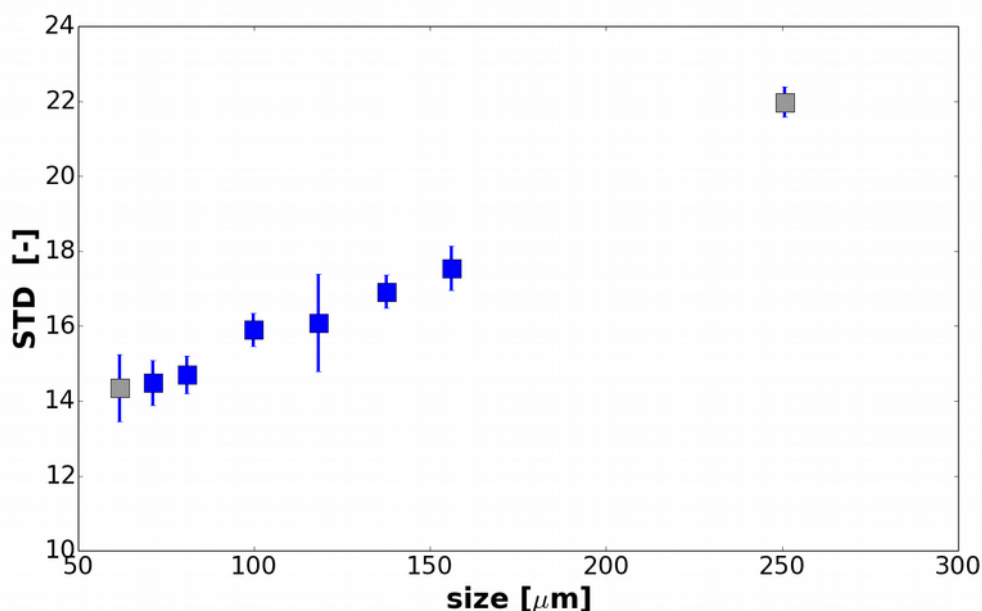


Figure 5: STD of the grey scale histogram of binary mixtures of MCC powder and granules as a function of the average particle size (bidispersed samples). Eight mixtures were analysed (0, 0.1, 0.2, 0.4, 0.5, 0.6, 0.8, 1.0 w/w). The two grey point refers to pure MCC powder and to pure granules.

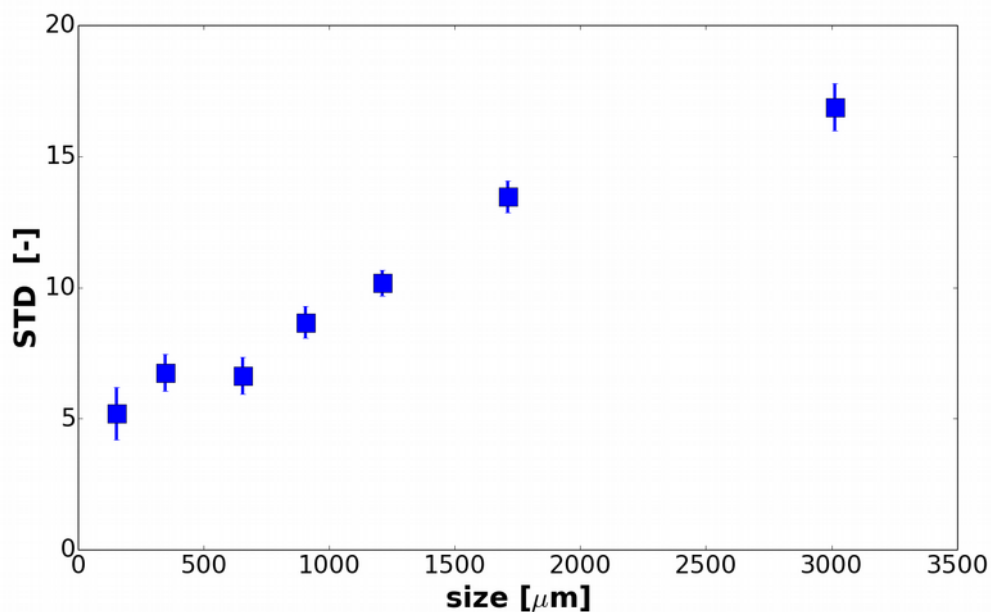


Figure 6: Dynamic analysis of the surface. STD of the gray-scale histogram as a function of the size.

S. Nalesso , C. Codemo, E. Franceschinis, N. Realdon, R. Artoni, A.C. Santomaso, Texture analysis as a tool to study the kinetics of wet agglomeration processes (2015) *International Journal of Pharmaceutics*, 485, 61-69.

DOI: <http://dx.doi.org/10.1016/j.ijpharm.2015.03.007>

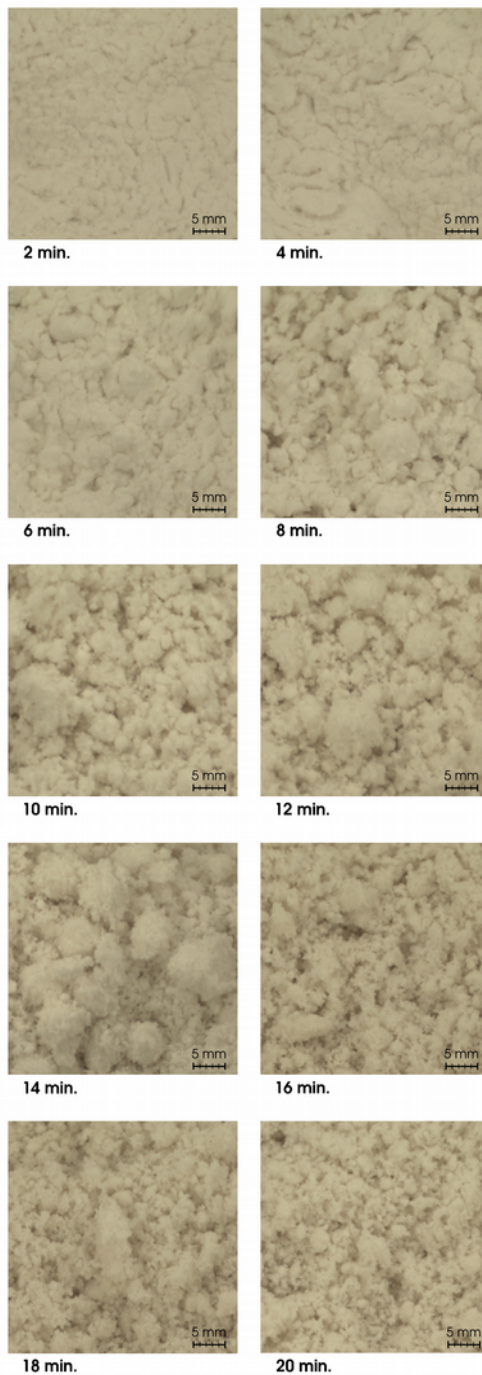


Figure 7: Evolution of the bed surface texture as a function of binder addition. The experiment was carried out at the following conditions: binder composition: 0.05% XG; binder addition rate: 28 ml/min; water amount: 330g.

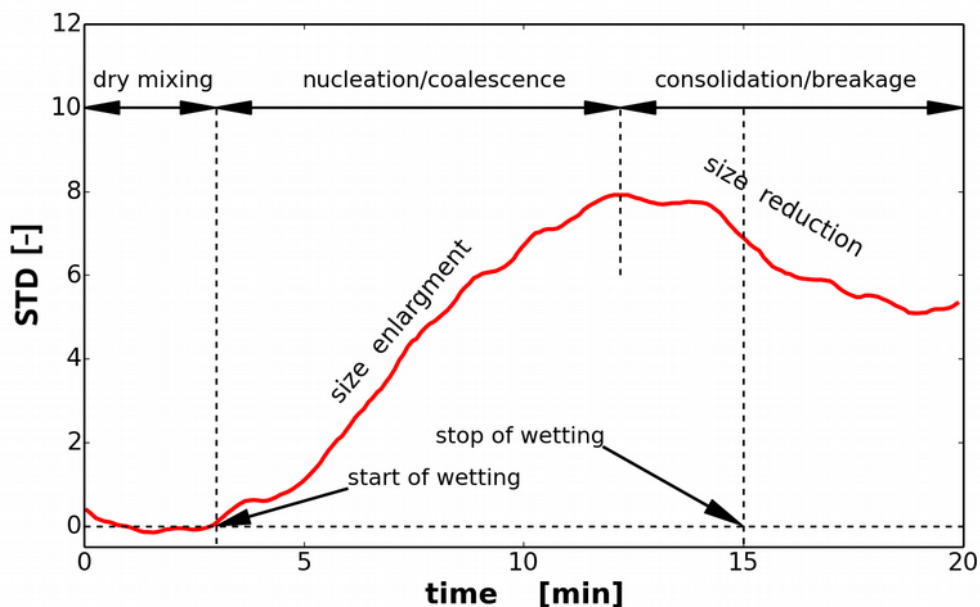


Figure 8: Typical profile of STD as a function of time during the granulation process.

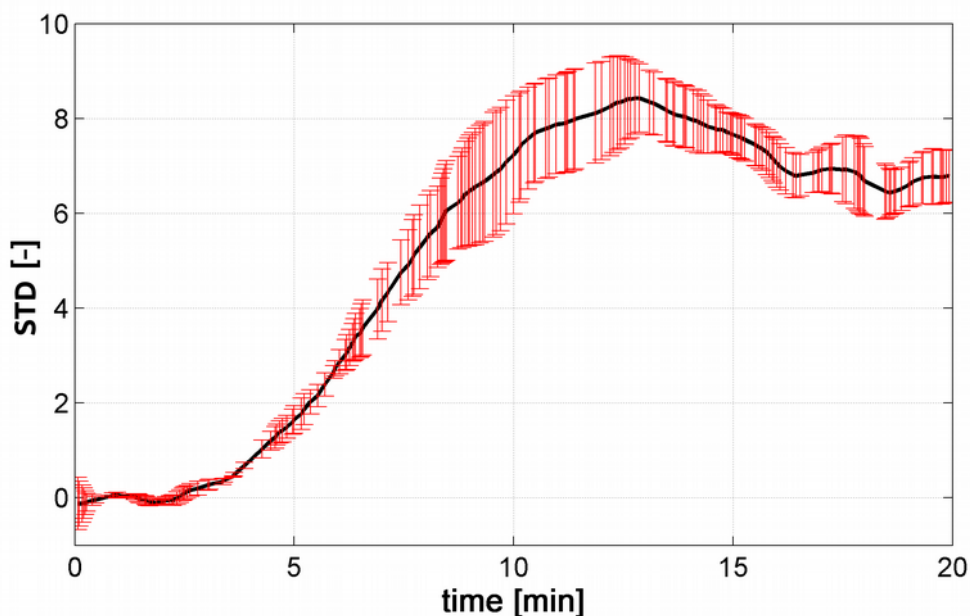
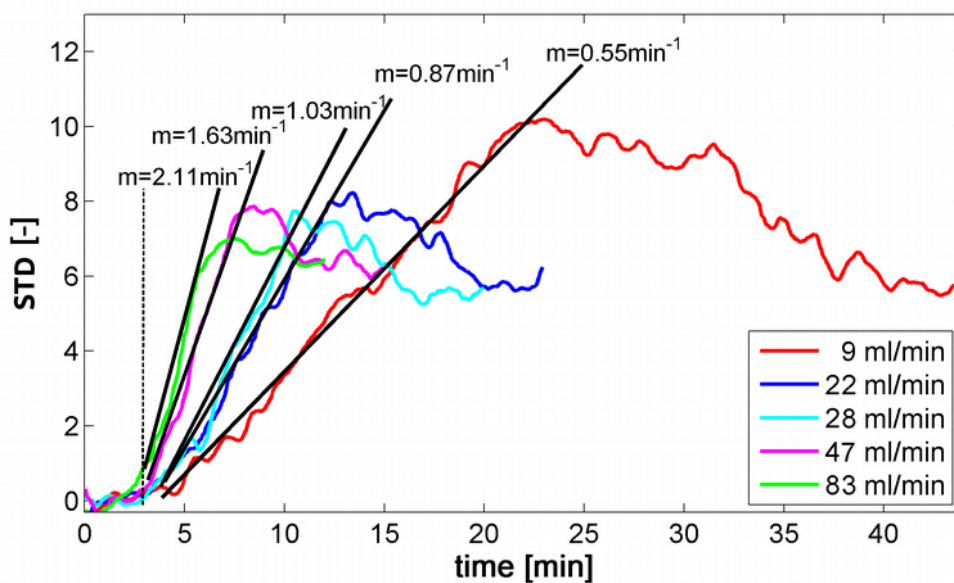


Figure 9: STD profile showing the typical variability of the granulation process and of the texture analysis.

a)



b)

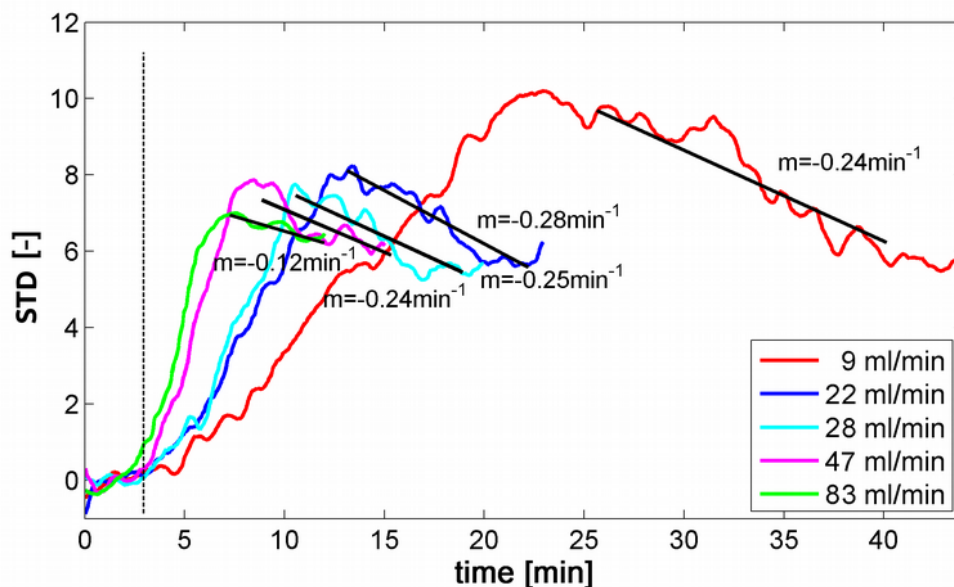


Figure 10: STD profile obtained for XG based binder (0.05 w/w%) at different flow rates and their linear interpolation in the size enlargement a) and size reduction b) stages.

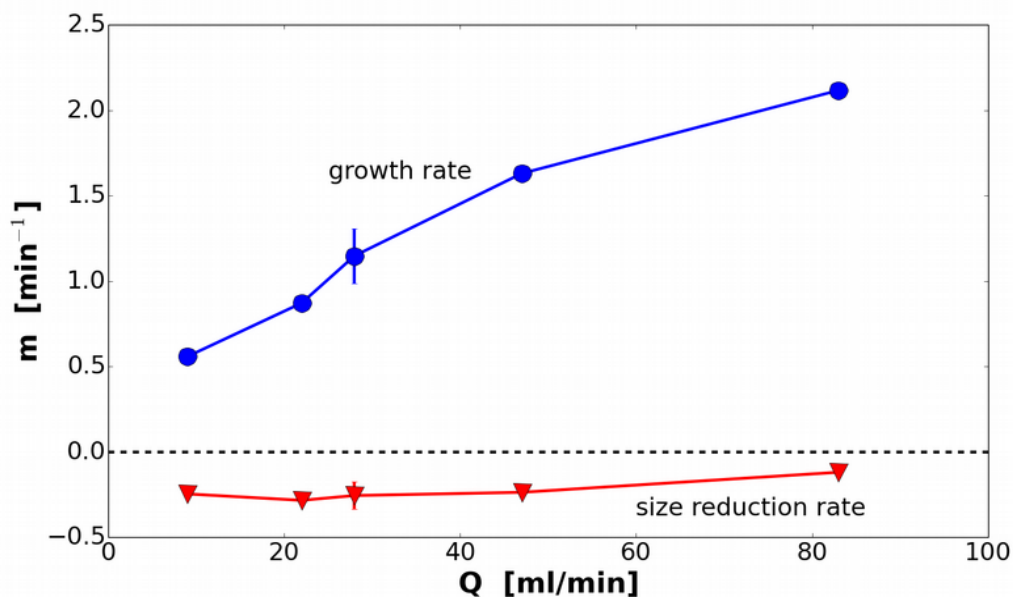


Figure 11: Kinetic constants m of the size growth and reduction as a function of the flow rate Q . Values are obtained from the slopes measured in Figure 10.

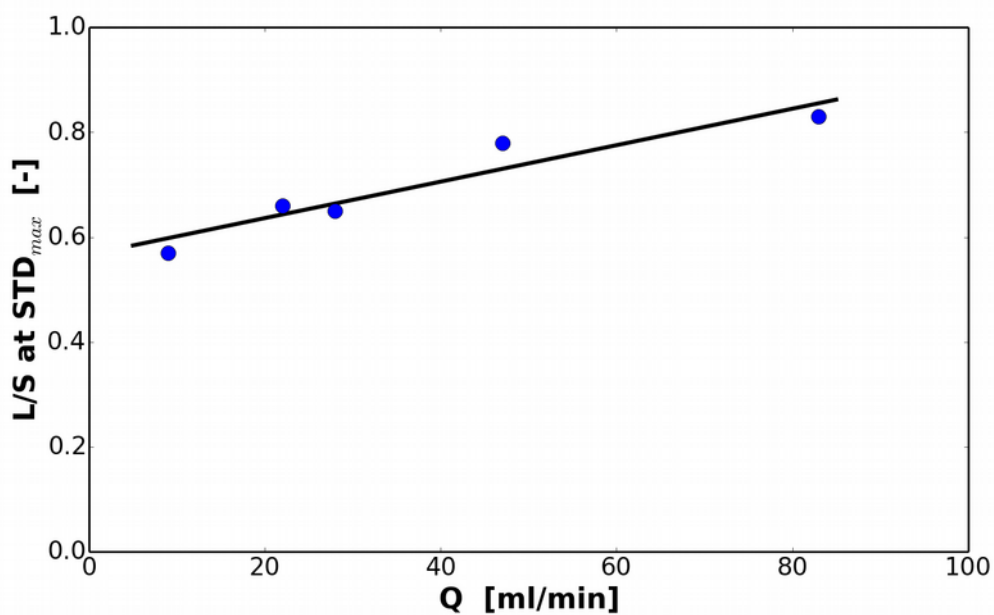


Figure 12: Liquid to solid ratio at the maximum of STD, as a function of the binder flow rate.

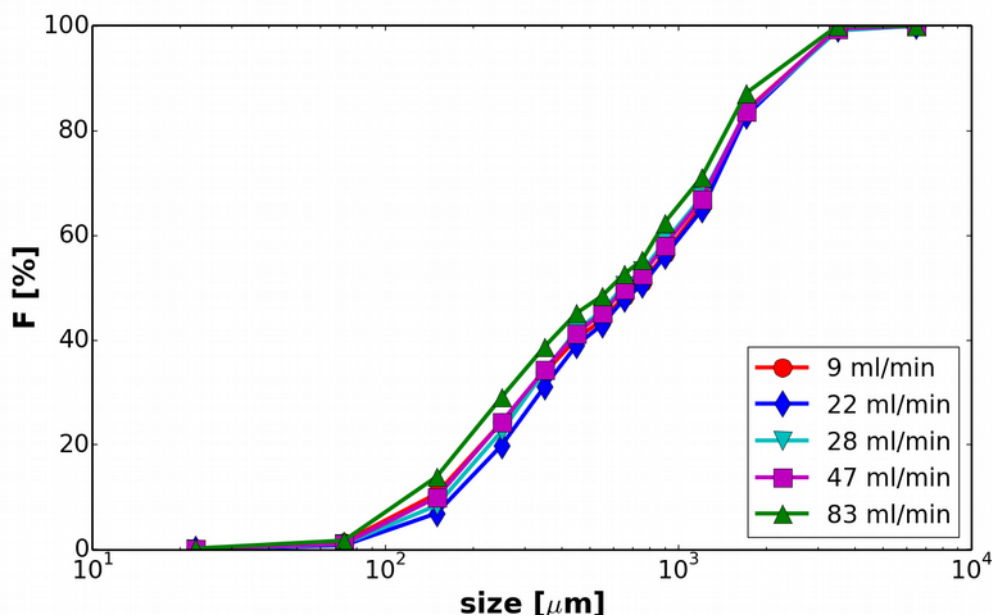


Figure 13: Cumulative mass fraction of granules obtained with dispersion of XG = 0.05% w/w at different flow rates.

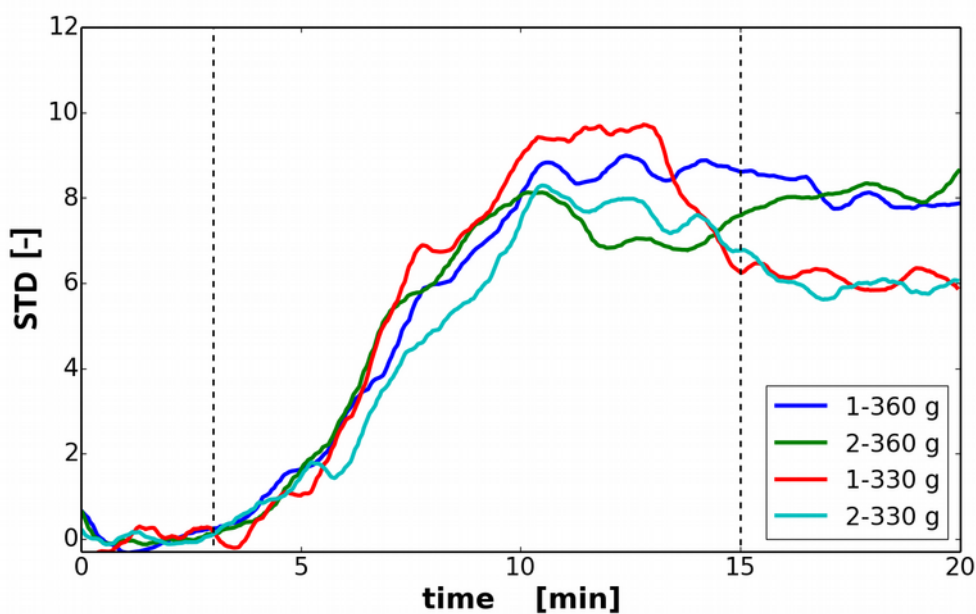


Figure 14: STD profiles for two different total amount of liquid binder (360 g and 330 g of binder respectively). Experiments have been replicated twice.

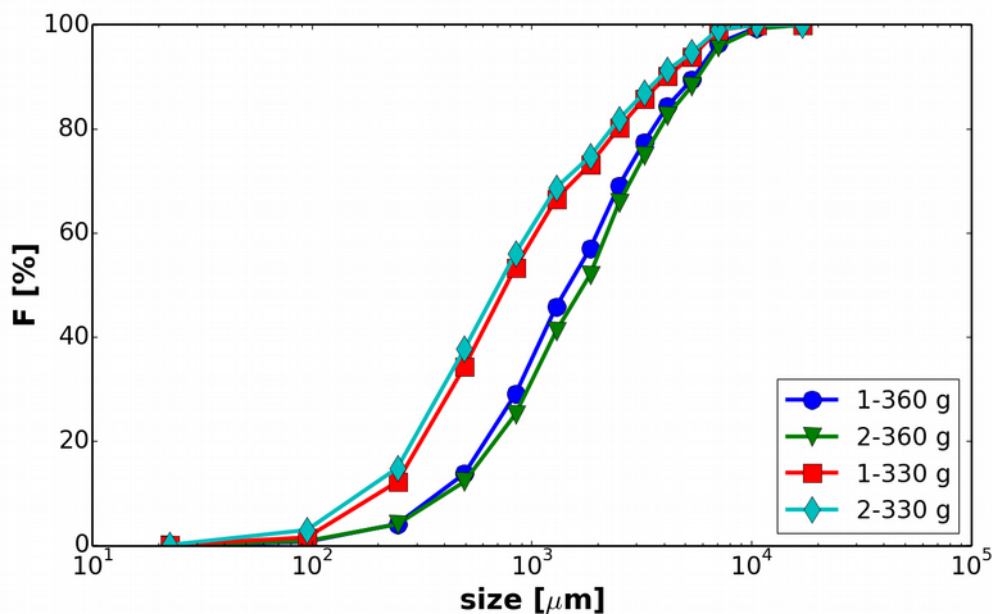


Figure 15: Cumulative mass fraction of granules prepared using two different amount of binder. XG=0.05% w/w.